J-10.4 Increased Interbed K_d of 78 mL/g

A mid-range interbed K_d of 50 mL/g was used in the RI/BRA model. As discussed in Section J-6, the expected interbed K_d range is 25-84 mL/g. The previous simulation presented in Section J-10.3 was presented to evaluate the low end of the range and used 22 mL/g. This sensitivity study examines the impact of using a K_d on the high end of the expected range, with this value equal to 78 mL/g.

J-10.4.1 Geochemical Evolution in the Alluvium

This sensitivity simulation uses the geochemical results obtained for the RI/BRA model presented in Section J-8. In the RI/BRA model, 12336 Ci were released in the first 20 years, with 3564 Ci remaining in the alluvium with a K_d of 2 mL/g. The difference between this simulation and the sensitivity base case is solely due to the increased interbed K_d, with this value equal to 78 mL/g.

J-10.4.2 Vadose Zone Sr-90 Simulation Results

The release of Sr-90 in this simulation followed the same procedure as was used in the RI/BRA model:

- 15900 Ci from CPP-31 release in the tank farm were represented using (a) the activity-release function shown in Figure J-8-9 (H) for the 12336 Ci released during the first 20 years, and placing this activity flux directly above the basalt interface of the base model (Appendix A, Section 5.1). The remaining 3564 Ci were placed roughly mid way through the alluvium, corresponding to the location of the peak measured soil concentrations obtained during the 2004 (Appendix G and Table 5-32) sampling cycle. To simulate the transport of the activity remaining in the alluvium, an effective K_d of 2 mL/g was used (Figure J-10-16 (J)) for the alluvium sediments.
- transport of Sr-90 from sources other than CPP-31 originating in the alluvium, whose location is spanned by the submodel (Appendix A, Section 5.1), were simulated using the submodel. Because these source locations were outside the influence of the high ionic strength, acidic CPP-31 release, a K_d of 20 mL/g was used in the submodel alluvium.
- transport of Sr-90 from sources located outside of the submodel horizontal extent were also placed in the base model used to simulate the transport of the CPP-31 remaining in the alluvium. The effective K_d for the alluvium underlying these source locations was also set to the value used to simulate the transport of Sr-90 predicted to remain in the alluvium after 20 yrs (first bullet). The relative magnitude of these sources are small relative to the residual Sr-90 predicted to remain in the alluvium after 20 yrs.

The distribution of Sr-90 in the vadose zone is shown in Figures J-10-39 through J-10-42 for the 1979-2293 time period. The arrival of Sr-90 in key perched water wells is compared to field data in Figure J-10-43, and is summarized for all wells in Figure J-10-44. The subplots presented in Figure J-10-43 shows that the model is still slightly overpredicting concentrations in the northern upper shallow perched wells. The match to wells in the south has been much improved. The match to field data worsens as the distance from the well to the tank farm, or the well from the percolation pond increases. This is because the higher K_d does not allow the Sr-90 to migrate outward from the higher concentration regions near these two source locations. It is likely that a very good match could be obtained with a slightly higher K_d and higher anthropogenic water losses in northern INTEC.

Peak vadose zone concentrations through time are shown in red in Figure J-10-45 and are about equal to those obtained using the RI/BRA model parameters (black). This is because the highest pore water concentrations are in the alluvium (and not affected by the interbed K_d), or that they are representative of the pore water in the basalts, which are also not affected by interbed K_d.

The rate at which Sr-90 enters the aquifer (red) is given in Figure J-10-46, and can be compared directly to the RI/BRA model results (black). As when the interbed K_d was assumed to be on the low end of the plausible range, using an interbed Kd on the high end of the range has had a significant impact on the expected migration rate of Sr-90 into the aquifer. Migration rates with this higher Kd are significantly higher throughout the entire simulation period. The distribution coefficient is essentially the ratio of mass (activity) adsorbed on the exchange sites to that in the aqueous phase. As the K_d increases, the aqueous phase concentration decreases. Applying the larger K_d to all of the interbed sediments allows much more adsorption of total Sr-90 activity throughout the vadose zone, including the deeper interbeds affected by the failed CPP-03 injection well. The higher K_d retards the downward migration of Sr-90 and allows more decay to occur en route to the aquifer. The flux rate predicted using a K_d of 78 mL/g is much lower than predicted in the RI/BRA model.

Figure J-10-39. Sr-90 vadose zone concentration assuming an interbed K_d=78 mL/g (horizontal contours) (pCi/L) (MCL = thick red line, 10*MCL = thin red line, MCL/10 = black line).

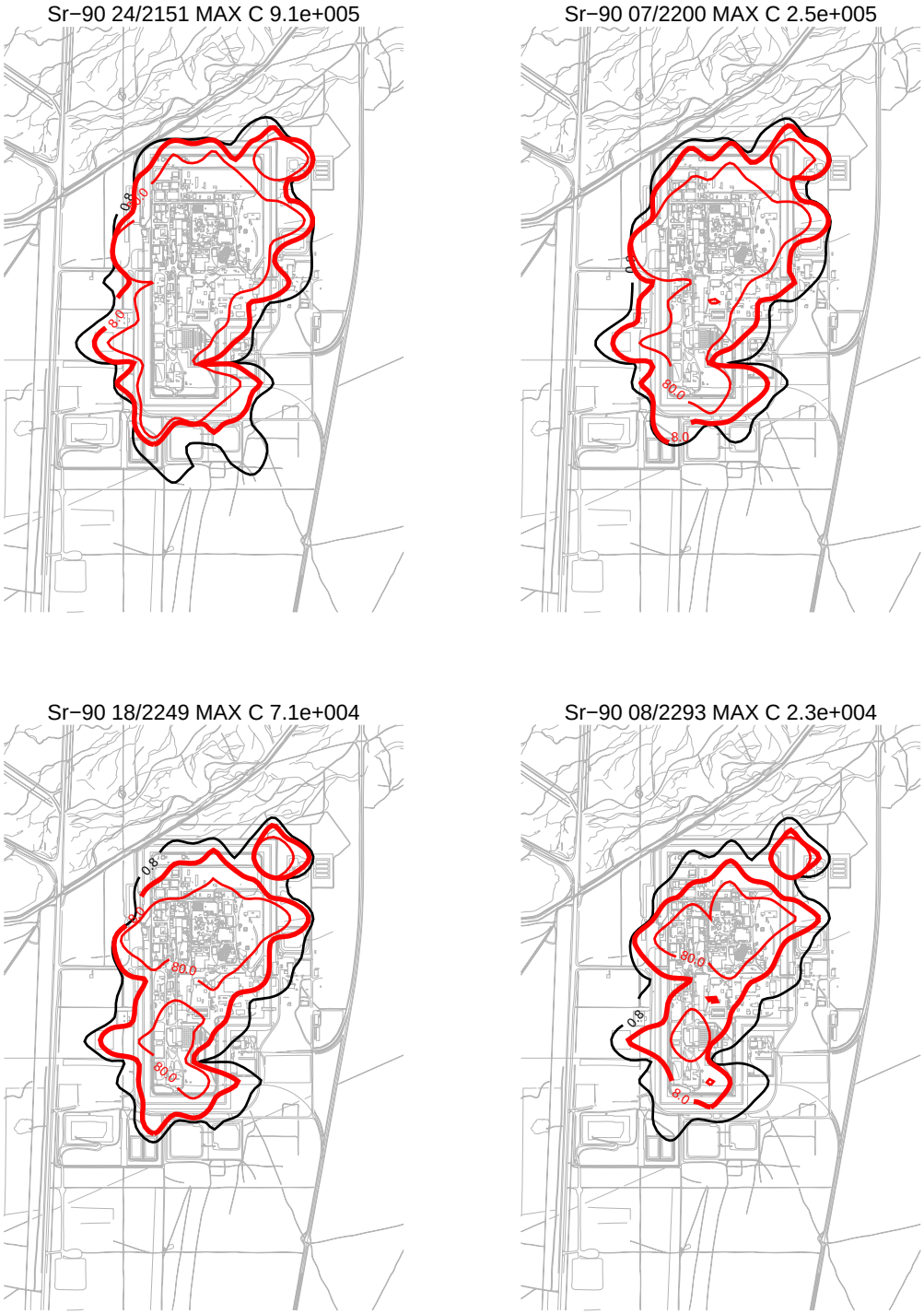

Figure J-10-40. Sr-90 vadose zone concentration assuming an interbed K_d=78 mL/g (horizontal contours) (pCi/L) (MCL = thick red line, 10*MCL = thin red line, MCL/10 = black line).

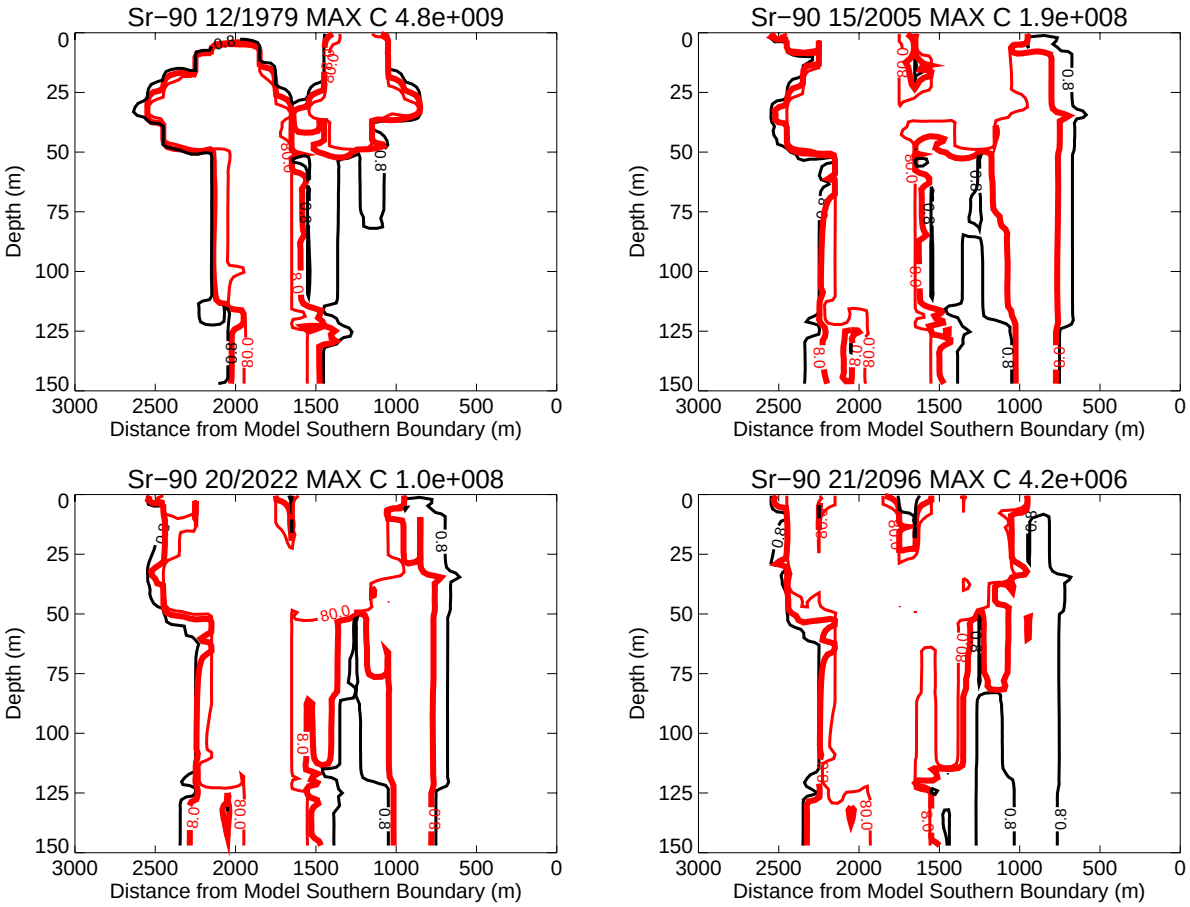

Figure J-10-41. Sr-90 vadose zone concentrations assuming an interbed K_d=78 mL/g (vertical contours) (pCi/L) (MCL = thick red line, 10*MCL = thin red line, MCL/10 = black line).

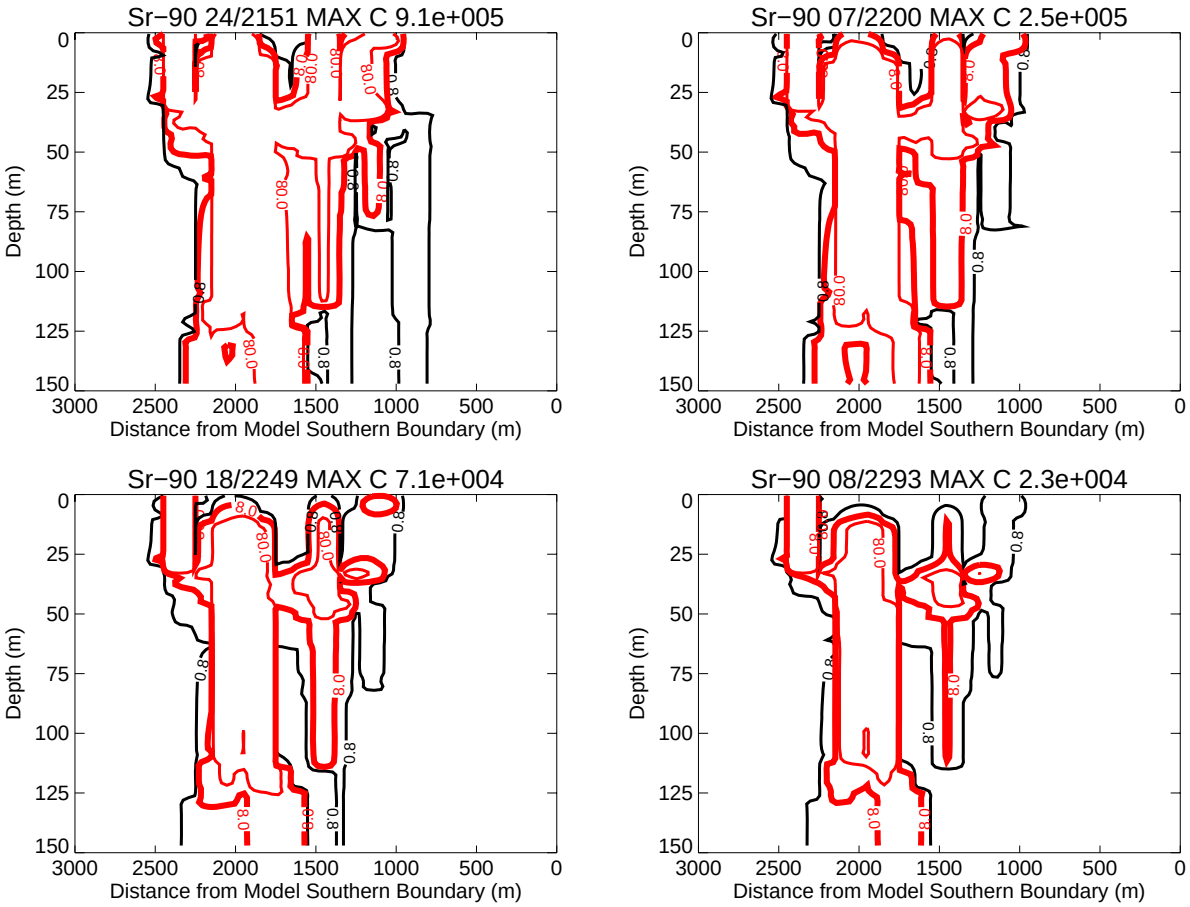

Figure J-10-42. Sr-90 vadose zone concentrations assuming an interbed K_d=78 mL/g (vertical contours) (pCi/L) (continued) (MCL = thick red line, 10*MCL = thin red line, MCL/10 = black line).

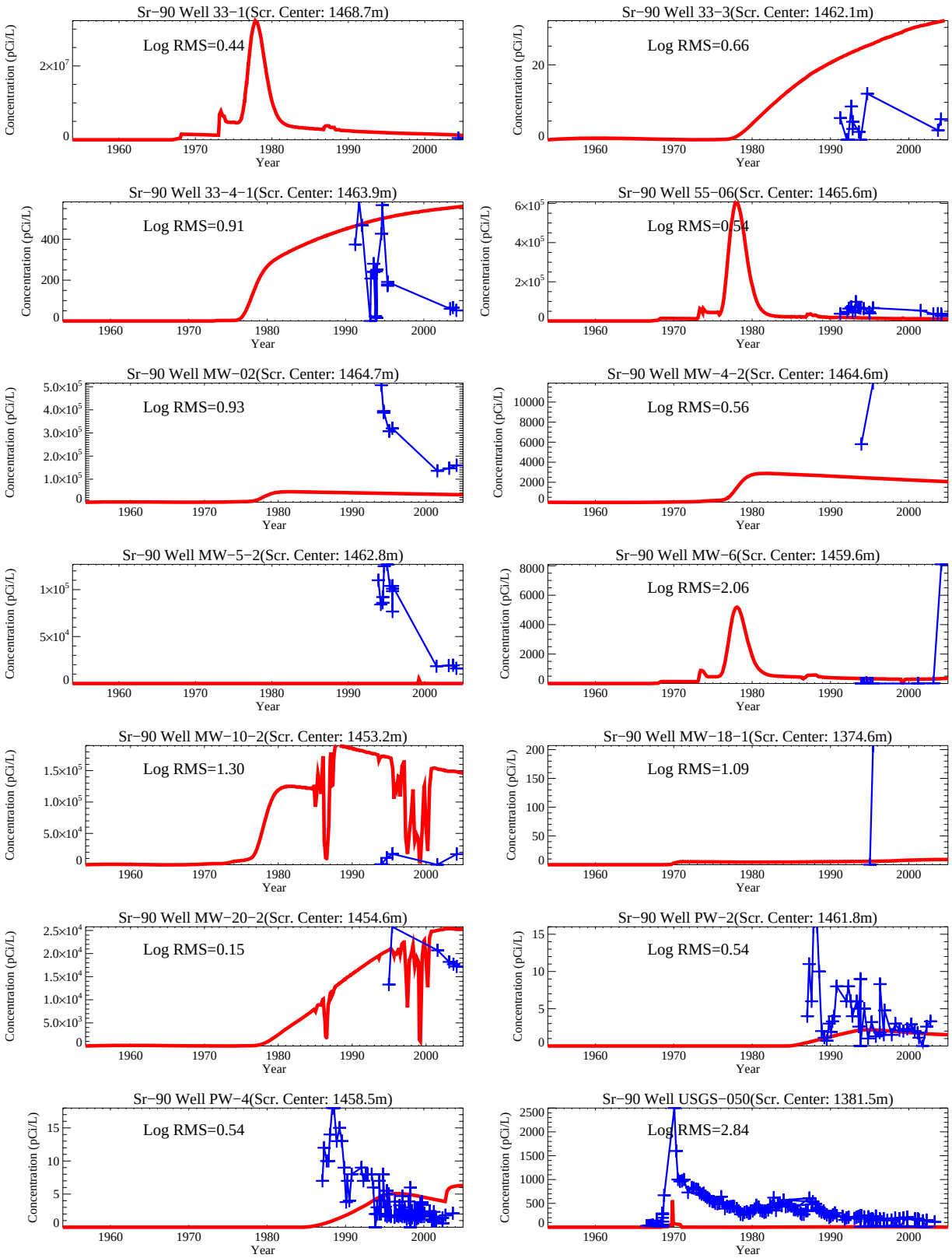

Figure J-10-43. Sr-90 concentration in perched water wells assuming an interbed K_d=78 mL/g (pCi/L) (Measured values = blue crosses, red = model at screen center).

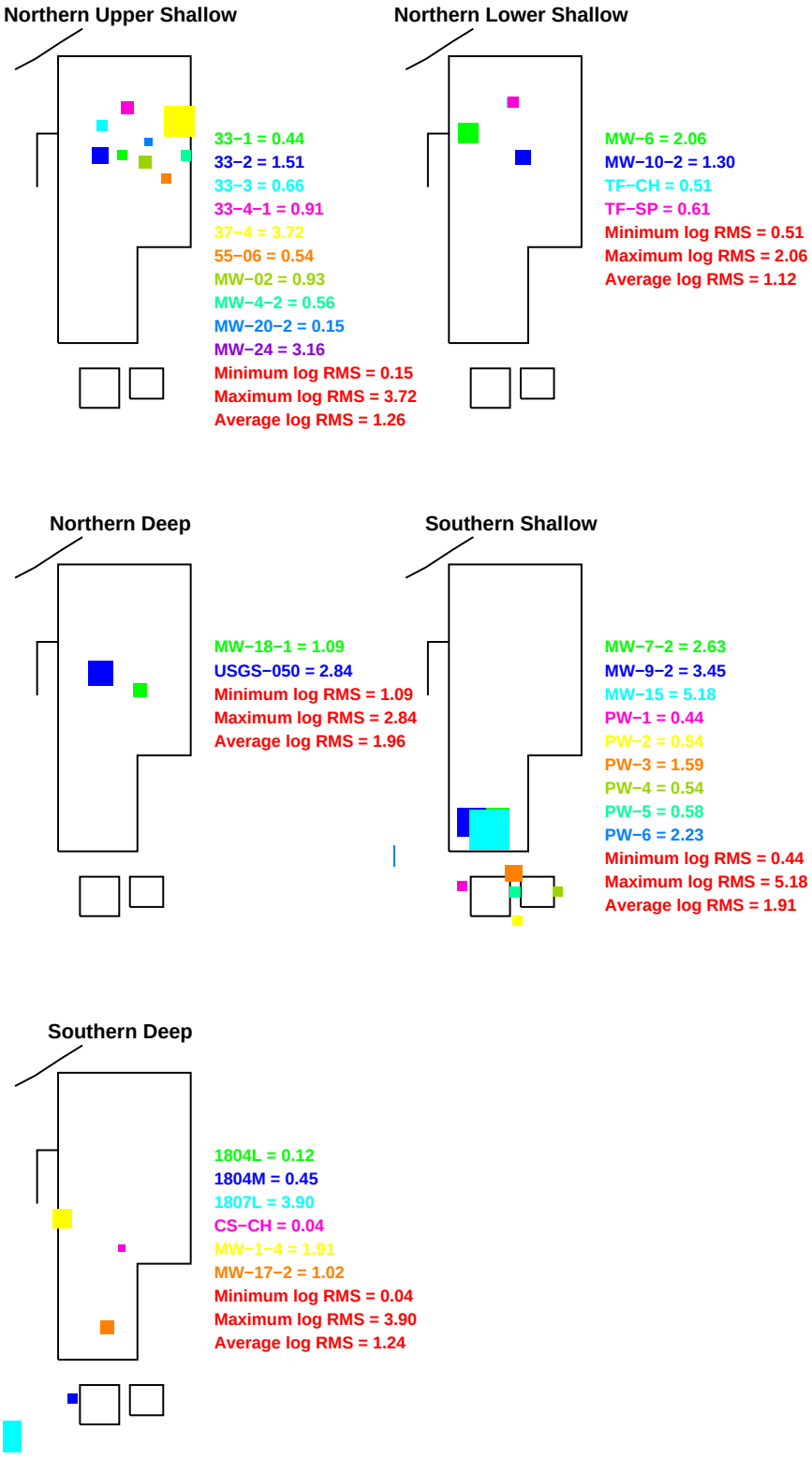

Figure J-10-44. Log 10 Root mean square error (RMS) by depth and northing assuming an interbed K_d=78 mL/g.

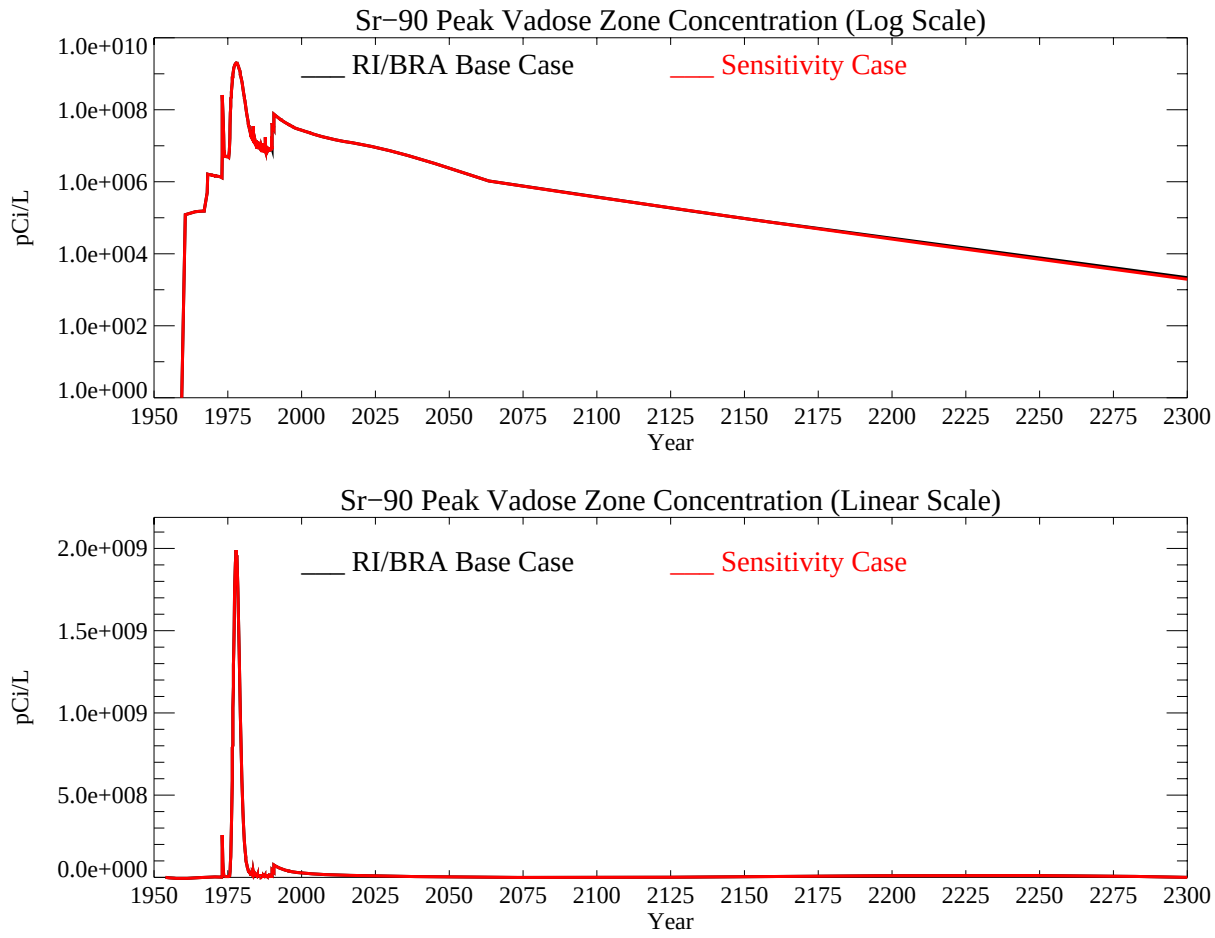

Figure J-10-45. Sr-90 peak vadose zone concentrations assuming an interbed K_d=78 mL/g (pCi/L) with the RI/BRA model in black and this sensitivity run in red.

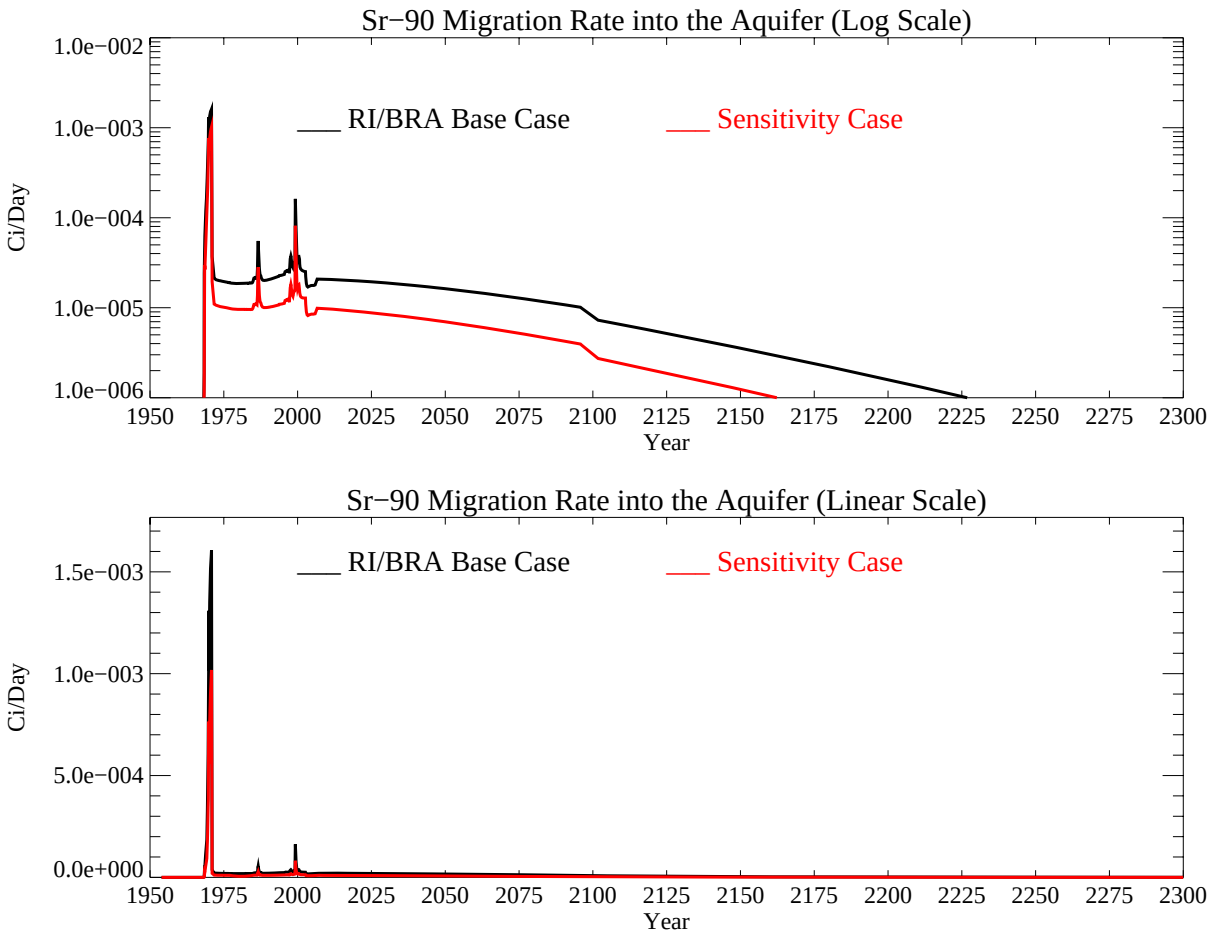

Figure J-10-46. Sr-90 activity flux into the aquifer assuming an interbed K_d=78 mL/g (Ci/day) with the RI/BRA base case in black, and this sensitivity run in red.

J-10.4.3 Aquifer Sr-90 Simulation Results

The distribution in Sr-90 in the aquifer for the time period spanning 2005-2096 is given on the course grid in Figure J-10-47. It is given for the 2049-2151 time period on the fine grid in Figure J-10-48. Resultant peak aquifer concentrations are given in Figure J-10-49. Because the Sr-90 originating in the vadose zone does not arrive in the aquifer until the mid 1980's, comparisons to measured data are not presented for aquifer wells.

The three performance measures are peak concentration in 2095, area impacted above the MCL, and time during which the MCL is exceeded. The peak concentration in 2095 is 8.1 pCi/L, about half that predicted for the RI/BRA base case (18.6 pCi/L). This difference is significant, but less than the difference predicted using a lower $K_{d.}$ given overall model uncertainty.

The more significant performance measure in this simulation is the spatial distribution of Sr-90. The Sr-90 contour plots presented in Figures J-10-47 and J-10-48 show that Sr-90 concentrations in the aquifer are predicted to exceed the MCL through year 2096. By year 2049, the region impacted by concentrations above the MCL are well within the INTEC fence line. This means that the flux rate of Sr-90 coming from the vadose zone is less than the dilution, retardation, and decay rate in the aquifer. It also implies that the source of Sr-90 south of INTEC in year 2022 is from the injection well or from earlier arrival of Sr-90 from the deep vadose zone impacted by that well's failure.

The simulated Sr-90 concentrations with this higher adsorption in the interbeds remain above the MCL from 1960 through year 2096. In the RI/BRA base-case, peak concentrations were not reduced below the MCL until year 2129.

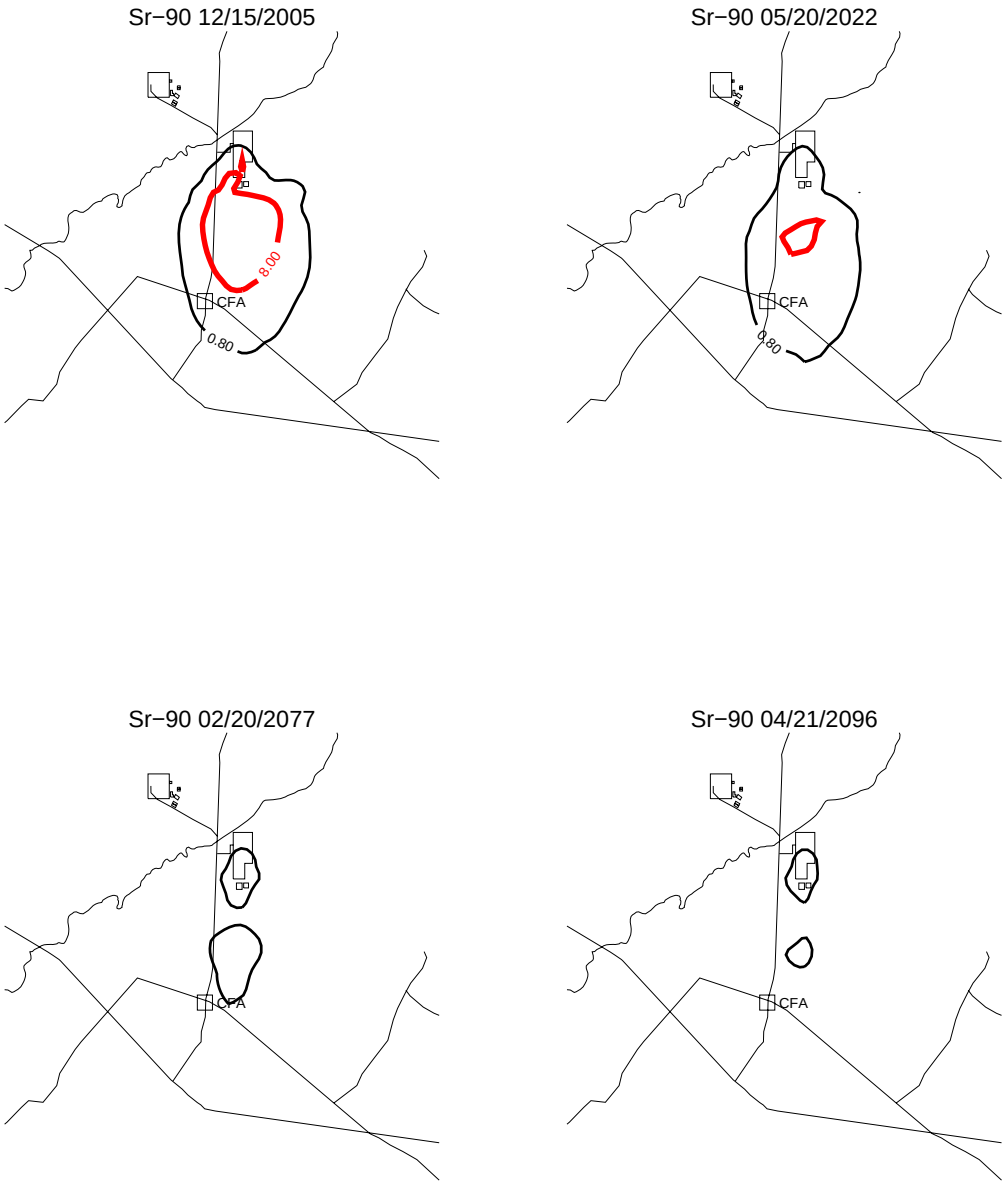

Figure J-10-47. Sr-90 aquifer concentration contours assuming an interbed K_d=78 mL/g (pCi/L) (MCL = thick red line, 10*MCL = thin red line, MCL/10 = black line).

Figure J-10-48. Sr-90 aquifer concentration contours assuming an interbed K_d=78 mL/g (pCi/L) (continued) (MCL = thick red line, 10*MCL = thin red line, MCL/10 = black line).

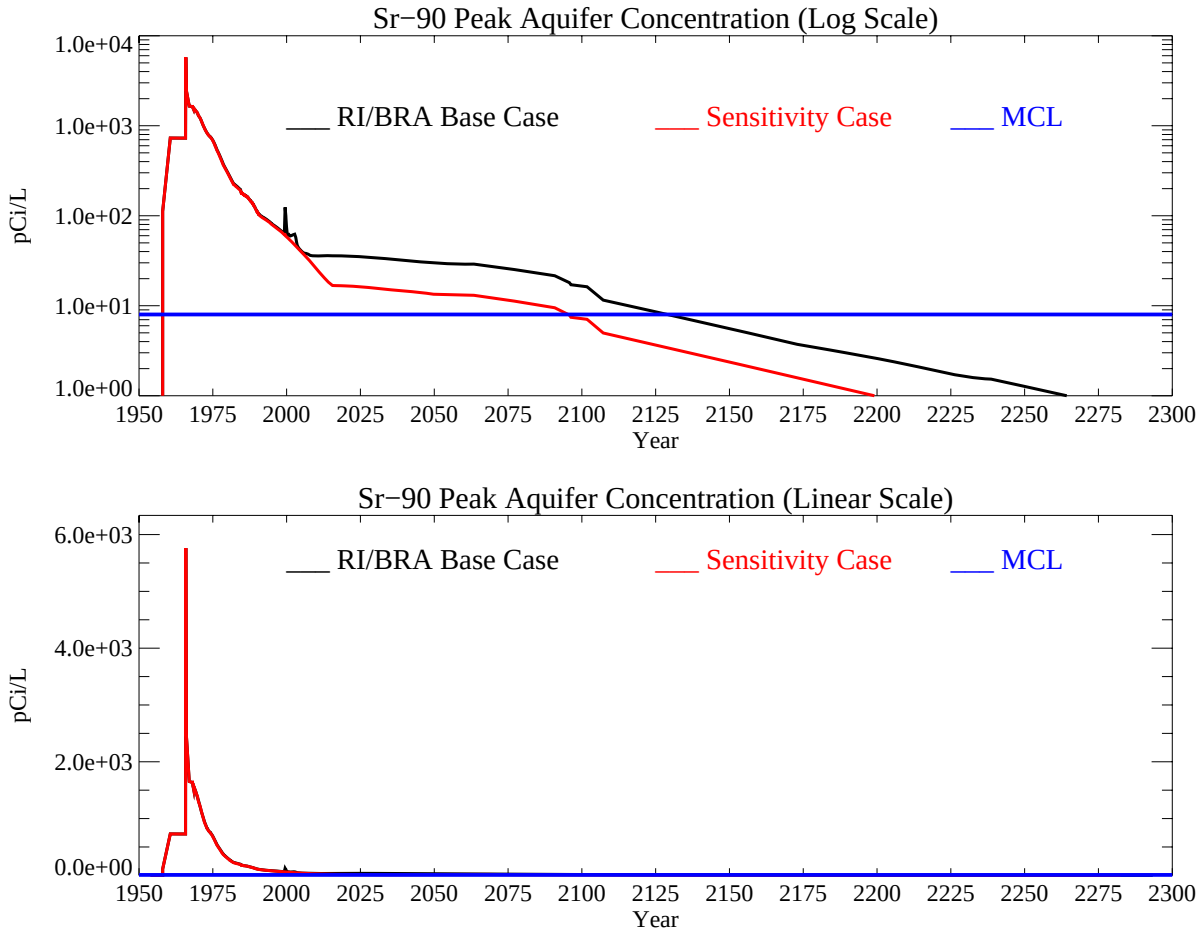

Figure J-10-49. Sr-90 peak aquifer concentrations assuming an interbed K_d=78 mL/g (pCi/L) with the MCL in blue, RI/BRA model in black and this sensitivity run in red.

J-10.5 Summary of Sensitivity to Geochemical Parameters

In the geochemical model, 15,900 Ci of Sr-90 were released to the alluvium by the CPP-31 leak. From the one-dimensional model, we saw that a fraction of the strontium moves relatively rapidly through the alluvium either complexed with nitrate ion, or because of inhibition of adsorption as a result of competition with elevated sodium and calcium concentrations in solution. Once the sodium-bearing waste peak has passed through the alluvium, the remaining strontium on the ion exchange sites is released much more slowly. With the parameters used in the model, the sodium-bearing waste pulse leaves the alluvium between 5 and 10 years after release. In all cases, we saw some fraction of the 15,900 Ci released within the first 10 years, with only a small incremental increase at 20 years (Table J-10-1).

In the 3-dimensional RI/BRA model, 12336 Ci of Sr-90 were released from the alluvium into the vadose zone after 20 years. As the CEC increases from 2 to 3 meq/100 g, the amount of Sr-90 released decreased slightly to 110864 Ci after 20 years. Increasing the CEC to 7 meq/100 g further decreased the amount of Sr-90 released at 20 years to 6403 Ci. From the simulated partitioning of strontium between liquid and solid phases we calculated K_d values (see Equation J-5-2) for the alluvium. There was quite a range in calculated partitioning coefficients (Table J-10-1). For CEC of 2 meq/100 g, K_d values are much lower than commonly considered applicable to alluvium. Higher K_d values at 7 meq/100 g were comparable to K_d values measured by the USGS.(Liszewski, et al. 1997; Liszewski, et al. 1998)

All of the CEC values used in the sensitivity runs were within the range of data obtained from the literature for INTEC alluvium. Changing the CEC produced two changes in model output. First, the fraction of the total Sr-90 released in the first 20 years was affected. Second, the steady-state K_d value after the leak has been flushed from the alluvium was affected. Decreasing the CEC resulted in more Sr-90 being flushed quickly from the alluvium. It also resulted in the remaining Sr-90 being more mobile. Higher CEC resulted in more Sr-90 being retained in the alluvium. However, the steady-state K_d value was higher so that this residual Sr-90 was less mobile. The amount of residual Sr-90 and the mobility of the residual Sr-90 are important for evaluating risk and remedial alternatives. The amount of Sr-90 released from the alluvium in the first 20 years affects perched water concentrations, and impacts the parameter values necessary for the vadose zone model to match measured Sr-90 concentrations in perched water.

The chemical composition of the pore water was estimated from measurements taken in perched water zones (Table J-3-4). These measurements reflect multiple sources of water, some of which contain contaminants or dissolved solids from plant water systems. Recharge in the alluvium is likely to be closer in composition to precipitation, and may have lower concentrations of sodium. Because sodium is one of the cations important in the competitive cation exchange reactions, the sensitivity of strontium transport to a lower sodium concentration in pore water/recharge was assessed. The other components in pore water are based on the assumption of calcite saturation at a partial pressure of carbon dioxide of 10^{-2} atm. This assumption fixes carbonate, pH, and calcium within a fairly narrow range. As a result, there is a limited range in uncertainty for calcium and pH and we did not test for sensitivity to these parameters.

The sodium concentration used in the pore water model is the lowest measured in perched water, and is equal to the concentration of sodium in the Snake River Plain aquifer. Precipitation may have a lower concentration. Sensitivity to sodium concentration was tested by dropping the sodium concentration to 0.22 mmol/L from 0.33 mmol/L in the base case. The change in sodium concentration resulted in a very slight increase in the release of Sr-90 at 20 years (Table J-10-1). The likely reason for this is that the lower background sodium concentrations increase the calcium saturation on the ion exchange sites. The greater fraction of calcium on the clays decreases the partitioning of strontium to ion exchange sites. This decrease is small and does not increase the release of Sr-90 significantly. Therefore, the Sr-90 release is not sensitive to background concentrations of sodium in the pore water and the estimated values used in the model do not need to be refined.

The third parameter evaluated for effect on Sr-90 release is the strontium selectivity coefficient. The selectivity coefficient is primarily related to the properties of the cation. Cations in solution are not equally sorbed to ion exchange sites on clays. Cations with greater hydrated ionic potential are preferentially sorbed. This means that divalent cations are more strongly bound than monovalent cations. Larger cations (greater atomic number) in a group are less strongly hydrated than smaller cations. As a result of the lower hydration, cations with greater atomic number have fewer waters of hydration and consequently a greater hydrated ionic potential. Thus, the order of preference for divalent alkaline earth cations is $Ba^{2+} > Sr^{2+} > Ca^{2+} > Mg^{2+}$. Strontium will be more strongly sorbed to ion exchange sites than calcium and magnesium as well as the monovalent cation sodium.

We varied the selectivity coefficient of strontium to be as low as calcium and as high as barium. Given the general consensus on the ordering of selectivity coefficients, this effectively brackets the total range over which the selectivity coefficient could range. We lowered the selectivity of strontium to a value (0.45) slightly lower than calcium. This increased the release of Sr-90 to 9,454 Ci because calcium and sodium were much more effective at competing for exchange sites with strontium. Raising the selectivity coefficient to a value more representative of barium decreased the release of Sr-90 to 3,369 Ci at 10 years. The calculated release of Sr-90 is sensitive to the selectivity coefficient for strontium. The range of selectivity coefficients tested exceeds the likely range in uncertainty in the selectivity coefficient because if the values selected were true, it would alter the selectivity sequence for cations. Furthermore, the selectivity coefficients used in the base case do a good job of matching laboratory measurements of strontium sorption to INTEC sediments. Therefore, we conclude that additional refinement of selectivity coefficients for INTEC specific materials is not likely to significantly impact the uncertainty in the calculated Sr-90 release from alluvium.

The final parameter investigated was the interbed K_d. Available field data suggests that a range of K_d in the interbeds would be appropriate. The range is dictated by soil textural and mineralogic characteristics in combination with water chemistry. Based on available data, this range spans 25 to 84 mL/g for sedimentary interbeds at the INL. At the low end of 22 mL/g, the RI/BRA model was used to predict peak concentrations of 110.8 pCi/L in year 2095, with concentrations falling below 8 pCi/L in year 2263. Near the high end of this range, a K_d of 78 mL/g results in a peak aquifer concentration of 8.1 pCi/L in 2095, with concentrations below 8 pCi/L by year 2096. Using the three performance measures of peak 2095 concentration, extent of the aquifer contaminated above the MCL, and the time during which concentrations exceed the MCL as a basis for comparison, the sensitivity of this model to interbed K_d is very high. Selecting a single value from the possible range helps bracket the endpoints of prediction, but in reality, a single value is unlikely to exist. Had spatially variable values been used, the peak concentration range would be narrower, converging to a value representative of the mean 50 mL/g K_d used in the RI/BRA model

Table J-10-1. Geochemical parametric sensitivity summary. All Sr-90 activities are undecayed.

	CEC=2 (meq/100 g)	CEC=3 (meq/100 g)	CEC=5 (meq/100 g)	CEC=7 (meq/100 g)	$K_{Na/Sr}$= 0.25	$K_{Na/Sr}$= 0.45	Na^+ = 0.22 (mmol/L)	CEC=2 (meq/100g) K_d=22 (mL/g)	CEC=2 (meq/100g) K_d=78 (mL/g)
Alluvium Statistics									
Years after CPP-31	**Activity Leaving Alluvium (Ci)**								
5 yrs	5187	4239	2793	1773	1658	3090	1921	5187	5187
10 yrs	12272	10820	8352	6378	3369	9454	6497	12272	12272
15 yrs	12310	10842	8368	6393	3373	9470	6509	12310	12310
20 yrs	12336	10864	8380	6403	3378	9480	6517	12336	12336
Activity Remaining in Alluvium (Ci)	3564	5036	7520	9497	12522	6420	9383	3564	3564
Effective K_d (mL/g) at 20 years	2	3.75	9.2	17	39	13		2	2
Vadose Zone Statistics									
Peak Concentration (pCi/L)	1.8E9	1.8E9	1.6E9	1.1E9				2.0E9	2.0E9
Year Peaked	1979	1979		1971				1978	1978
Aquifer Statistics									
Peak Concentration (pCi/L) in 2095	18.6	16.7		11.5				110.8	8.1
Year C is below 8 pCi/L	2129	2123		2105				2263	2096

shaded cells = RI/BRA base case

J-11 SENSITIVITY TO HYDROLOGIC CONDITIONS

Sensitivity to hydrologic conditions was determined through simulation using the base model discussed in Section J-8. In these sensitivity simulations a single parameter change was made. The RI/BRA base model was based on an alluvium CEC of 2 meq/100 g, a strontium selectivity coefficient of 0.35, a background sodium concentration of 3.3 mmol/L, an average infiltration rate of 18 cm/yr, and an interbed K_d of 50 mL/g.

- The first sensitivity to hydrologic conditions includes simulations using an initial infiltration rate of 18 cm/yr through the first 5 years after the CPP-31 release at which time, the infiltration rate was reduced to 2 cm/yr in order to account for the infiltration reducing liner that was placed on the tank farm in 1977.
- As discussed in Appendix A, Section 3.3 and in Appendix B, it is not clear that the liner is effective in reducing infiltration through the tank farm, and some of the monitoring results suggest that it may be increasing local recharge in that area. The second sensitivity simulation evaluates the transport using an infiltration rate of 39 cm/yr to account for that potential increase in infiltration rate. As with the first hydrologic sensitivity run, the rate was not changed until year 1977.
- In the base case simulations for all of the contaminants evaluated in this RI/BRA, it was assumed that the water losses due to anthropogenic activities were distributed throughout INTEC. It is likely that more of these water losses occur in northern INTEC in association with increased facility activity. The fourth sensitivity examines the effect of higher recharge in northern INTEC.
- The fifth hydrologic sensitivity is presented to examine the effect of removing the anthropogenic water altogether after year 2035. Clearly, the influence of recharge is large, as evidenced by the sharp reduction in flux rates into the aquifer from the vadose zone shortly after year 2095. This sharp reduction was apparent in each of the activity-flux into the aquifer plots presented thus far. There is an ongoing effort to reduce the anthropogenic water losses at INTEC. If this effort is effective, those losses will occur much earlier than the 2095 time-frame assumed for the base-case simulations. This simulation is presented to evaluate the importance accelerating actions to reduce anthropogenic water losses.
- The sixth sensitivity is presented to evaluate the potential land-use impact. In the RI/BRA, it was assumed that the land-use through year 2095 would require pumping water from the SRPA at current rates. This assumption is consistent with an industrial use scenario, where large water volumes would be necessary in order to sustain the commercial activities. If the land-use changes significantly, or if the current production wells are moved out of the influence of INTEC (i.e., further north or east), the draw-down currently observed in the aquifer would stop. Pumping is assumed to stop in year 2012, 2035, and 2096 in the three scenarios evaluated.
- The final sensitivity simulation examines the effect of increasing the interbed dispersivity in an attempt to better match concentrations in wells to the southeast of the tank farm. In most of the results presented this far, predicted concentrations in wells to the southeast have been lower than observed. Achieving the lateral migration necessary to move the Sr-90 toward those wells might be possible by increasing the lateral dispersivity.

These results are summarized in Table J-11-1 following the presentation of simulation results for each case.

J-11.1 Lower 3 cm/yr Infiltration Through The Tank Farm Liner

The RI/BRA model incorporated infiltration from precipitation at a rate of 18 cm/yr applied within the INTEC fence line including through area representing the tank farm. Five years after the CPP-31 release, an infiltration reducing liner was placed over the tank farm. In this simulation, we assume that from the beginning of the simulation period through 1976 the infiltration rate through the tank farm is 18 cm/yr. In 1977 and beyond, we assume that the liner is effective at reducing infiltration to 3 cm/yr in the four grid blocks representing the tank farm. This total 3 cm/yr implies that anthropogenic water leaks and precipitation infiltration are reduced by the presence of the liner.

J-11.1.1 Geochemical Evolution in the Alluvium

A decrease from 18 cm/yr to 3 cm/yr in infiltration rate occurring 5 years after the CPP-31 release has resulted in a rapid decrease in SrCO3 and SrOH in the aqueous phase, accompanied by an increase in Sr+ ion in the aqueous phase. The relative abundance of Sr+ ion is much larger than that of SrCO3 and SrOH, resulting in an increase in aqueous phase Sr-90 concentrations with the decrease in infiltration water. This is presumably a result of decreasing the incoming flux of Na, HCO3-, and Ca+2 ions that are contained in the infiltration water.

The amount of transported aqueous-phase Sr-90 is somewhat sensitive to this change in buffering capacity, and as a result, more Sr-90 leaves the alluvium in the first 20 years under this scenario than was predicted to occur in the absence of the tank farm liner. After 5, 10, 15, and 20 years, the total Sr-90 that has entered the vadose zone under the alluvium is 1342, 7243, 7845, and 8037 Curies, respectively as shown in Figure J-11-1. With this lower infiltration rate, a slightly smaller fraction (7863 Ci vs. 9497 Ci) remains in the alluvium after 20 years (Figure J-11-1). The flux rate shown in Figure J-11-1 (H) has an relatively high spike due to the numerical differentiation of the cumulative effluent shown in Figure J-11-1 (G) that is smoothed as the data is input into the vadose zone model.

The largest difference in the distribution of Sr-90, relative to the base case, occurs in the adsorbed Sr-90. Shortly after the decrease in infiltration rate, there is a rapid decline in Sr-90 on the exchange sites. The effective K_d is essentially the ratio of activity on the exchange sites to that in the aqueous phase. As the exchanged activity decreases, the aqueous phase Sr-90 concentrations increase, and the effective K_d decreases. The time evolution of this parameter is quite different than observed in the RI/BRA base case (Figure J-8-9 (J)). After 20 years, the effective K_d has not equilibrated to an average value as was observed in the other simulations, primarily because the decreased flux rate has not yet flushed the remaining sodium and calcium from the CPP-31 release out of the alluvium. Although not at a pseudo-steady state, at 20 years, the effective K_d is roughly 6.4 mL/g.

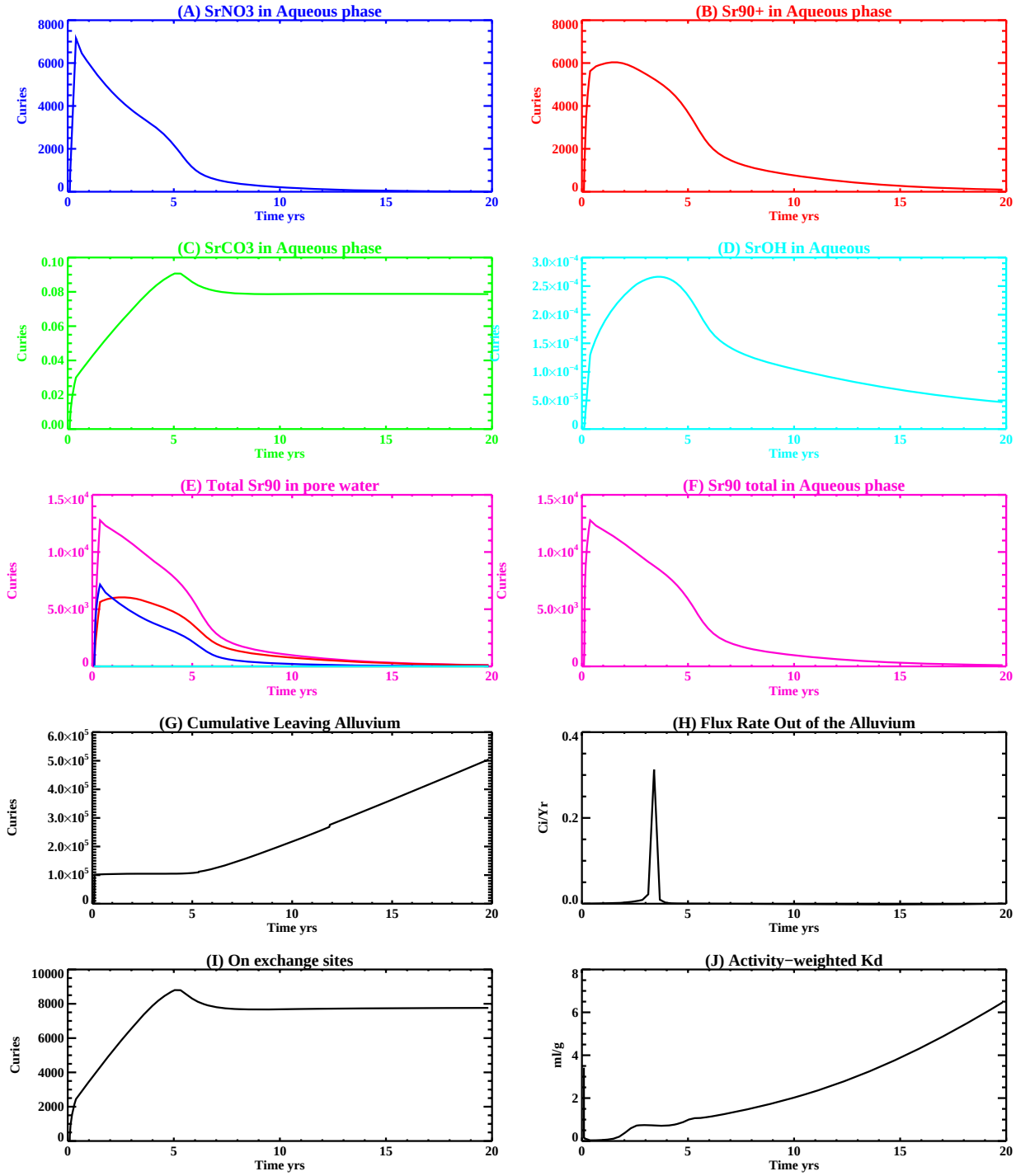

Figure J-11-1. Summary figure illustrating the speciation of Sr-90 in the aqueous phase (A-F), total Sr-90 in the pore-water of the alluvium (E), cumulative curies of Sr-90 having left the alluvium (G), flux rate leaving the alluvium (H), Sr-90 on the exchange sites (I), and effective partitioning coefficient (Kd) (J).

J-11.1.2 Vadose Zone Sr-90 Simulation Results

The release of Sr-90 in this simulation followed the same procedure as was used in the RI/BRA model:

- 15900 Ci from CPP-31 release in the tank farm were represented using (a) the activity-release function shown in Figure J-11-1 (H) for the 8037 Ci released during the first 20 years, and placing this activity flux directly above the basalt interface of the base model (Appendix A, Section 5.1). The remaining 7863 Ci were vertically through the alluvium, scaled to the measured soil concentrations obtained during the 2004 (Appendix G and Table 5-32) sampling cycle. To simulate the transport of the activity remaining in the alluvium, an effective K_d of 6.4 mL/g was used (Figure J-11-1 (J)) for the alluvium sediments.
- transport of Sr-90 from sources other than CPP-31 originating in the alluvium, whose location is spanned by the submodel (Appendix A, Section 5.1), were simulated using the submodel. Because these source locations were outside the influence of the high ionic strength, acidic CPP-31 release, a K_d of 20 mL/g was used in the submodel alluvium.
- transport of Sr-90 from sources located outside of the submodel horizontal extent were also placed in the base model used to simulate the transport of the CPP-31 remaining in the alluvium. The effective K_d for the alluvium underlying these source locations was also set to the value used to simulate the transport of Sr-90 predicted to remain in the alluvium after 20 yrs (first bullet). The relative magnitude of these sources are small relative to the residual Sr-90 predicted to remain in the alluvium after 20 yrs. In this case, the K_d is much lower than that used to simulate the transport of Sr-90 from sources within the submodel boundary. However, this should not effect the peak aquifer concentrations by more than 10%.

The distribution of Sr-90 is presented in Figures J-11-2 through J-11-5 for the 1979-2293 time period. The arrival in key perched water wells is compared to the field data in Figure J-11-6, and is summarized for all of the perched water wells in Figure J-11-7. The match to observed data in the key wells is quite similar to that obtained in the RI/BRA base case. In general, the match to field data with these parameters is slightly better in northern INTEC, and slightly worse in southern INTEC. The better match in northern INTEC results from the complex combination of reduced infliltration (anthropogenic and precipitation) causing less dilution and less Sr-90 being mobilized through the alluvium in the first 20 years following the CPP-31 release. Higher concentrations would be expected with less dillution, and lower concentrations would be expected with less Sr-90 present. In this case, the competing effects balance and allow the predicted concentrations in the perched water to be quite similar. The poorer match to southern wells is more informative. With an effecitve K_d higher than used in the RI/BRA base case, concentrations are less overpredicted. This is indicative of percolation pond water being of lower ionic strength, effectively raising the K_d from the base case value of 2 mL/g. It suggests that the effective K_d in southern INTEC should be in the 2-10 mL/g range.

Peak vadose zone concentrations through time are given in Figure J-11-8 in red, and are shown for the RI/BRA base case in black. As expected from the similarity in RMS, the peak concentrations are quite similar. The differences occur shortly after the liner emplacement, and are probably associated with pore water concentrations in the alluvium. The rate at which Sr-90 enters the aquifer from the vadose zone is given in Figure J-11-9 for this simulation in red, and can be compared directly to the RI/BRA base case (shown as black). It is interesting to note that the decrease in infiltration rate resulted in:

- 35% less Sr-90 leaving the alluvium in the first 20 years (8037 vs. 12336) following the alterations in chemical balance caused by reducing the influx of HCO_3 as discussed in Section J-11.1.1.
- twice as much Sr-90 remaining in the alluvium (7863 Ci vs.3564 Ci)
- decreased mobility of Sr-90 in the alluvium reflected by a larger K_d (6.4 mL/g vs. 2 mL/g)

The relatively low K_d used to simulate the transport of the Sr-90 remaining in the alluvium still allows most of the Sr-90 to remain in the alluvium. The small differences between flux rates into the aquifer for the RI/BRA base case and this simulation are due to the complex combination of reduced infliltration (anthropogenic and

precipitation reduced to 3 cm/yr) causing less dilution and less Sr-90 being mobilized through the alluvium in the first 20 years following the CPP-31 release. Higher concentrations would be expected with less dillution, and lower concentrations would be expected with less Sr-90 present. In this case, the competing effects balance and allow the predicted flux rates out of the vadose zone to be quite similar. The long-term persistence of the similarity is consistent with the results shown in Section J-9.4 where it was shown that with an alluvium K_d of 2 mL/g, leaving 3564 Ci of Sr-90 in the alluvium does not result in an appreciable increase the flux of activity leaving the vadose zone. In this case, the amount left in the alluvium after 20 years is only twice that amount, and the K_d in this case is three times higher.

Figure J-11-2. Sr-90 vadose zone concentration reducing infiltration in the tank farm to 3 cm/yr (horizontal contours) (pCi/L) (MCL = thick red line, 10*MCL = thin red line, MCL/10 = black line).

Figure J-11-3. Sr-90 vadose zone concentration reducing infiltration in the tank farm to 3 cm/yr (horizontal contours) (pCi/L) (MCL = thick red line, 10*MCL = thin red line, MCL/10 = black line).

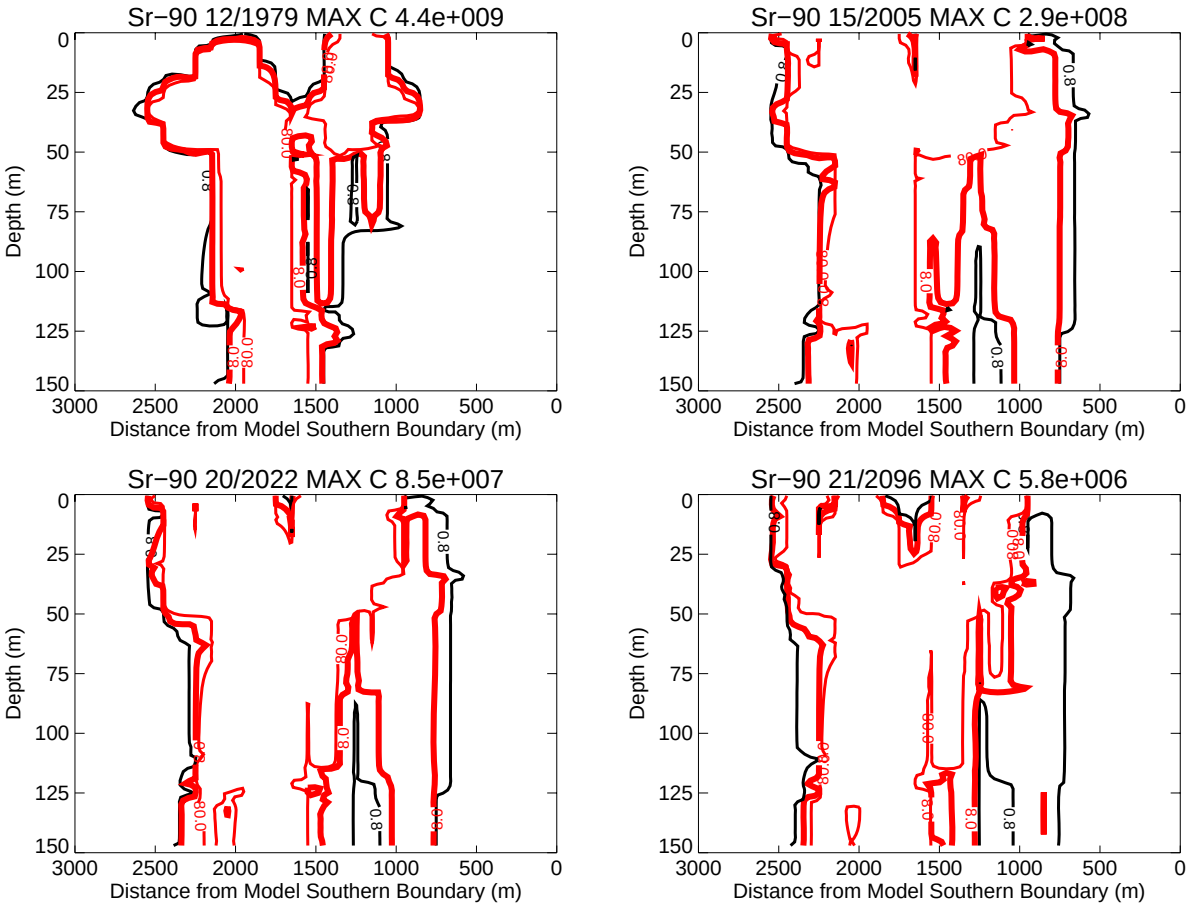

Figure J-11-4. Sr-90 vadose zone concentrations reducing infiltration in the tank farm to 3 cm/yr (vertical contours) (pCi/L) (MCL = thick red line, 10*MCL = thin red line, MCL/10 = black line).

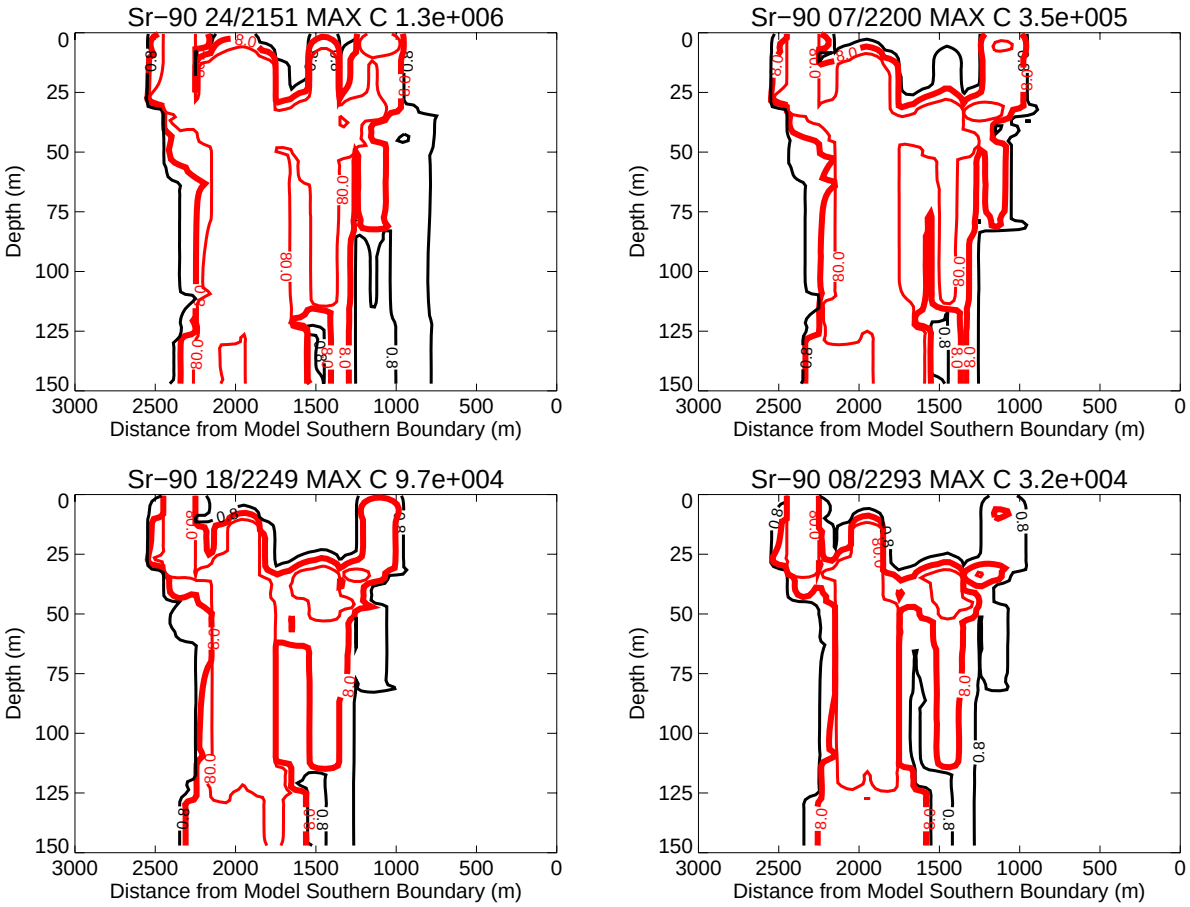

Figure J-11-5. Sr-90 vadose zone concentrations reducing infiltration in the tank farm to 3 cm/yr (vertical contours) (pCi/L) (continued) (MCL = thick red line, 10*MCL = thin red line, MCL/10 = black line).

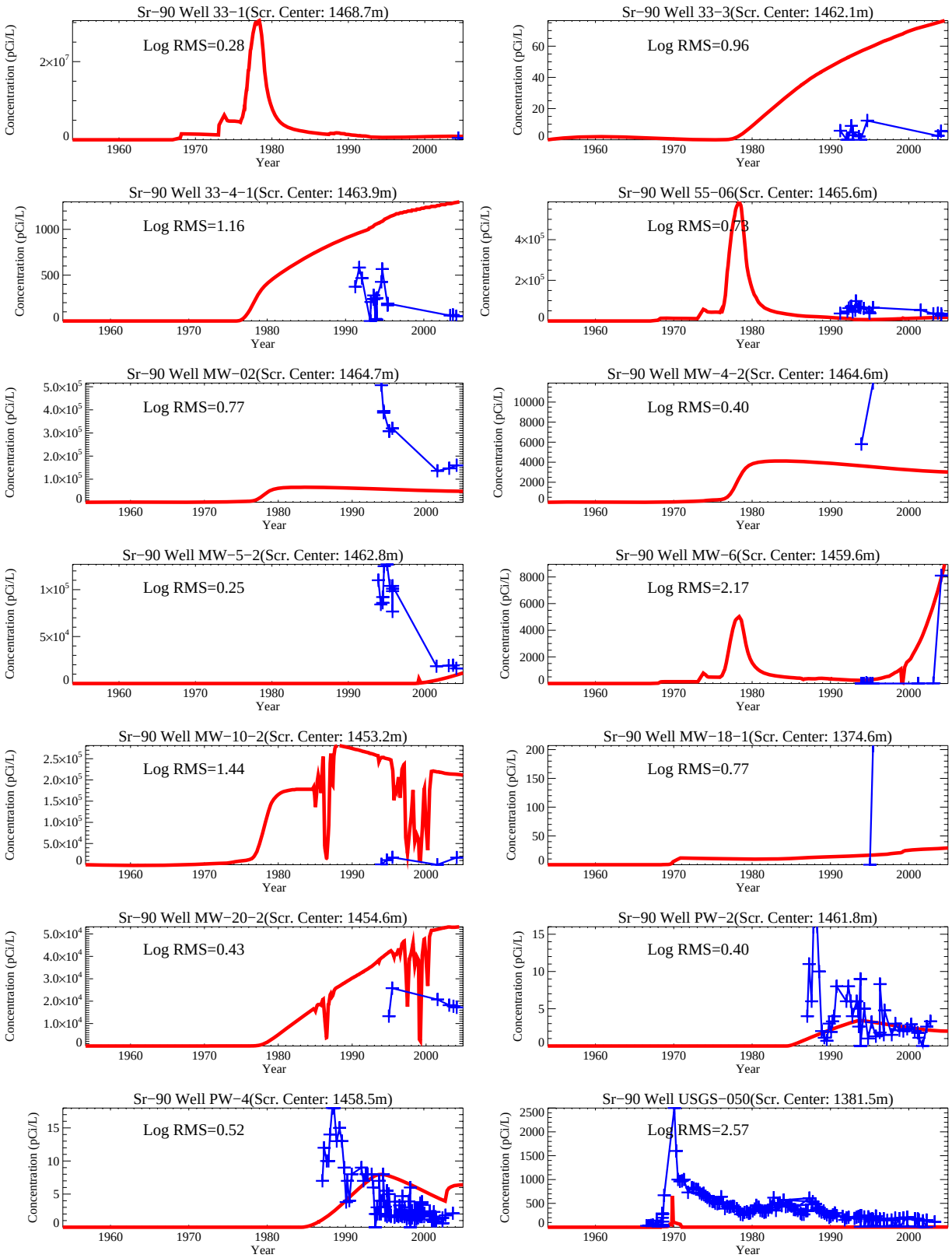

Figure J-11-6. Sr-90 concentration in perched water wells reducing infiltration in the tank farm to 3 cm/yr (pCi/L) (Measured values = blue crosses, red = model at screen center).

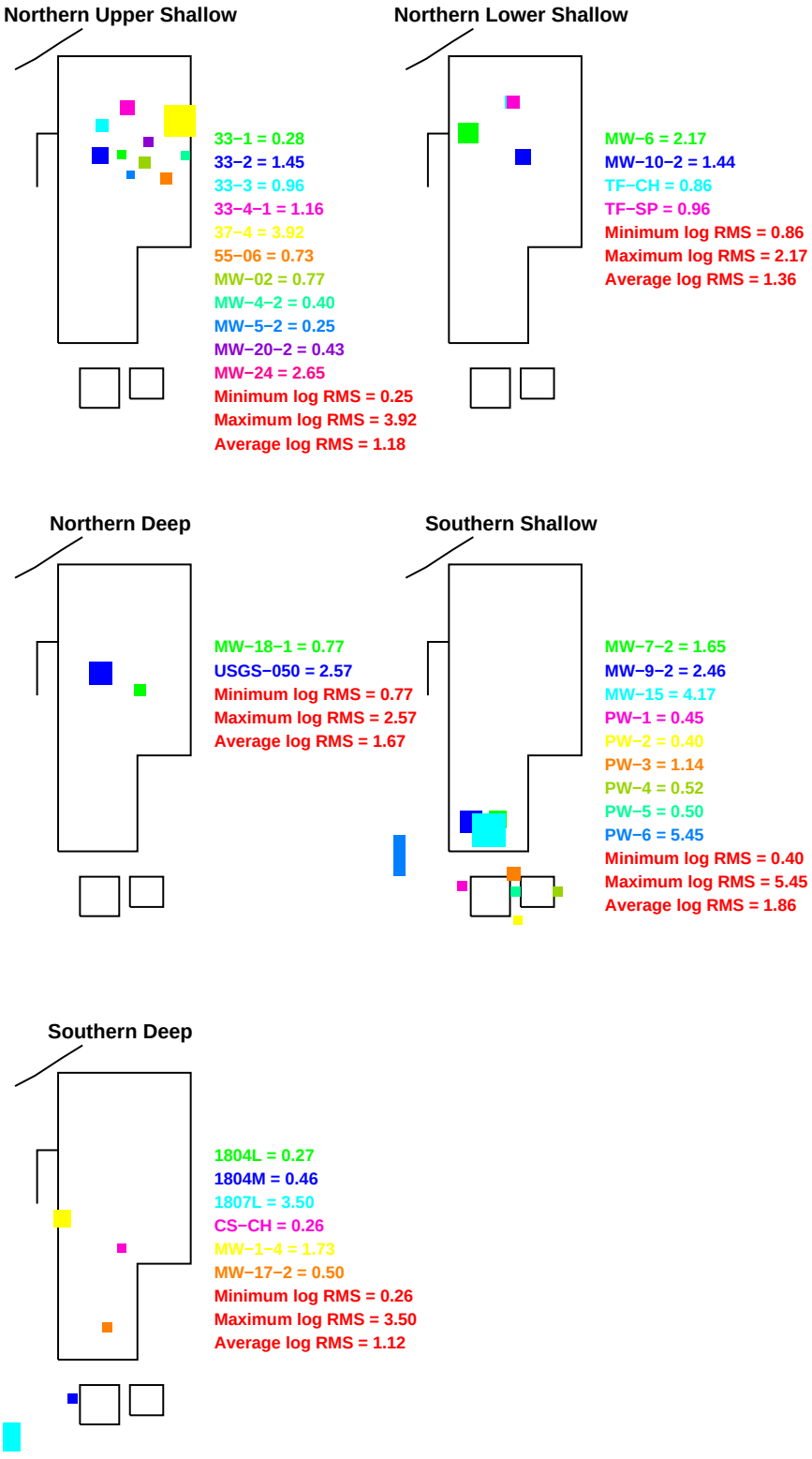

Figure J-11-7. Log 10 Root mean square error (RMS) by depth and northing reducing infiltration in the tank farm to 3 cm/yr.

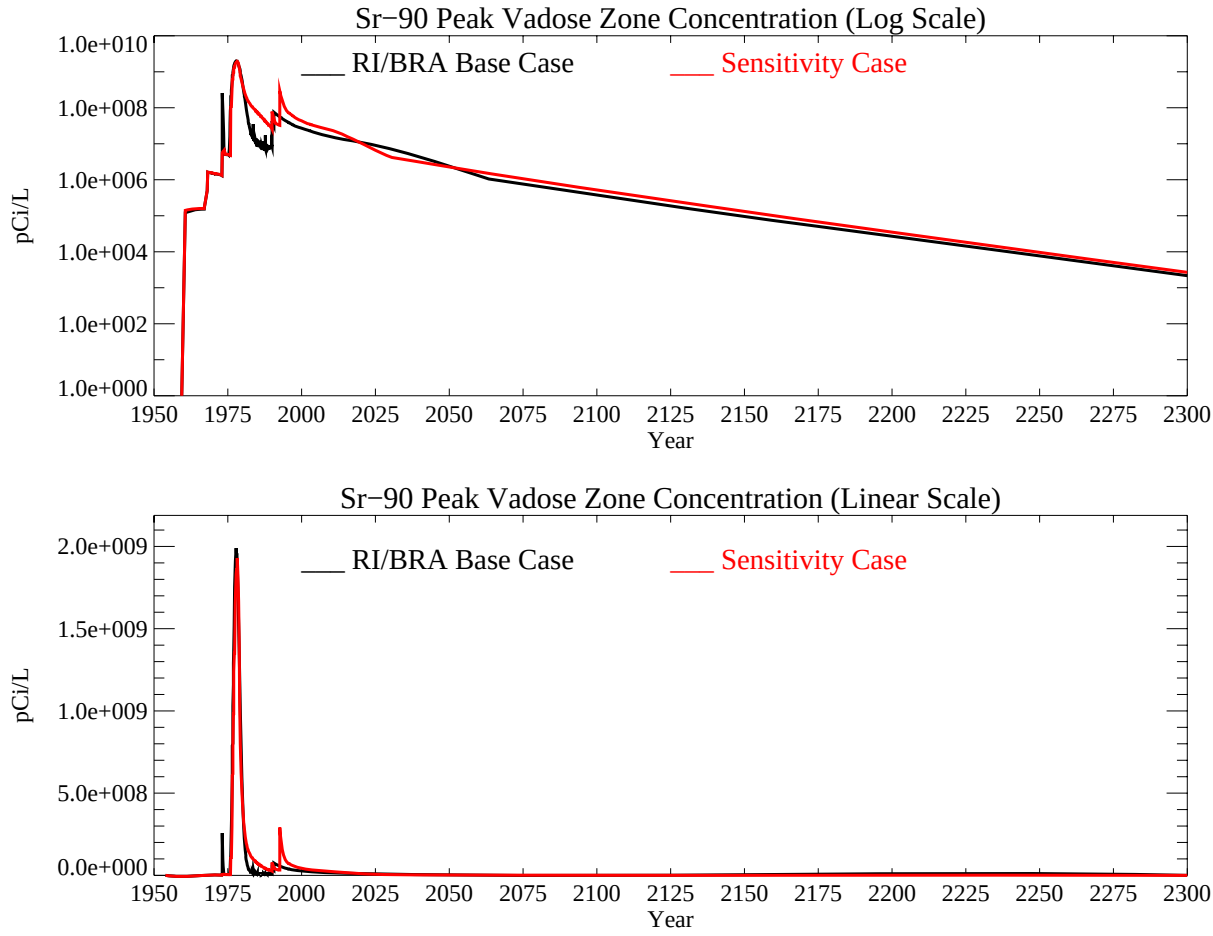

Figure J-11-8. Sr-90 peak vadose zone concentrations reducing infiltration in the tank farm to 3 cm/yr (pCi/L) with the RI/BRA model in black and this sensitivity run in red.

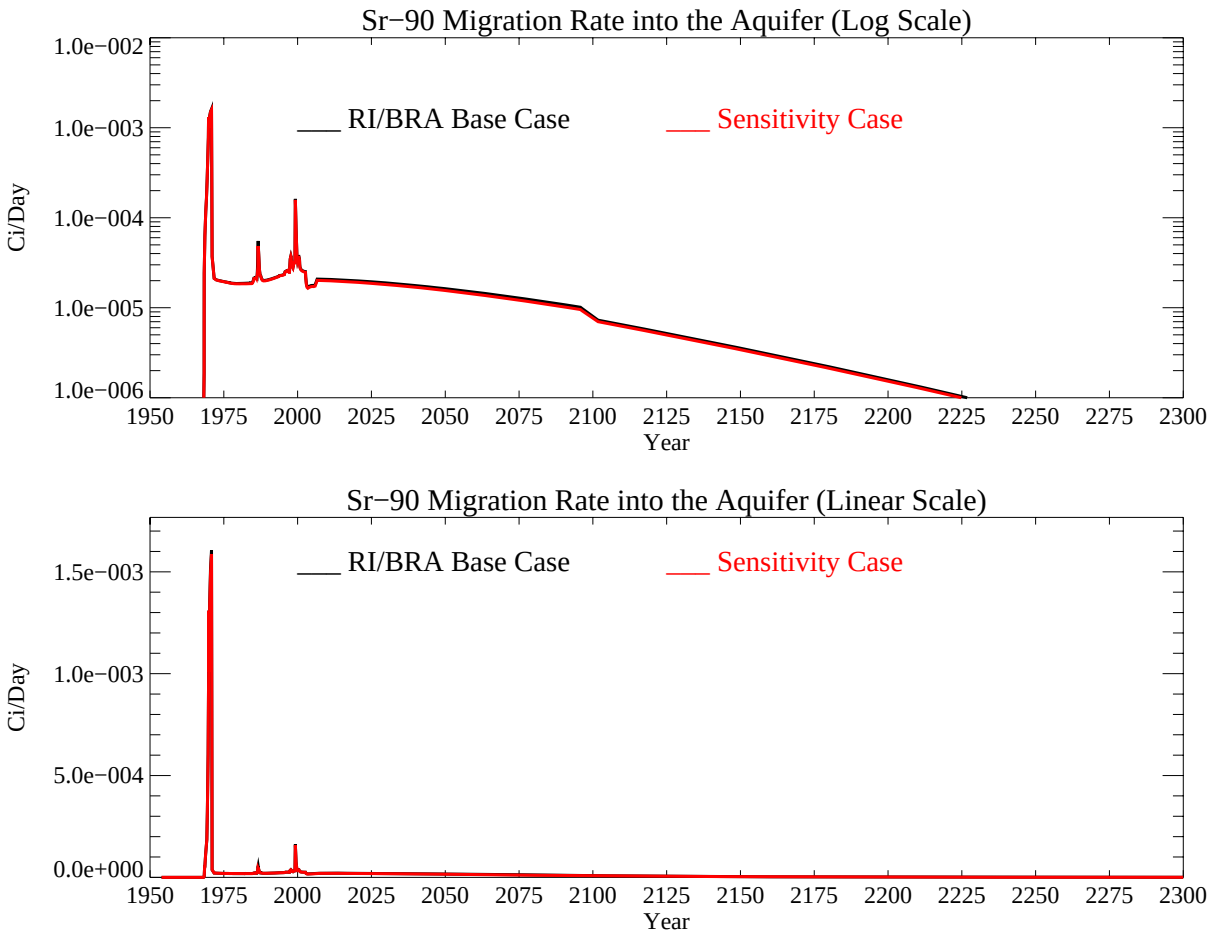

Figure J-11-9. Sr-90 activity flux into the aquifer reducing infiltration in the tank farm to 3 cm/yr (Ci/day) with the RI/BRA model in black and this sensitivity run in red.

J-11.1.3 Aquifer Sr-90 Simulation Results

The distribution of Sr-90 in the aquifer for the time period spanning 2005-2096 is given in Figure J-11-10 for the far-field with near-field results shown for the 2049-2151 time frame in Figure J-11-11. There are significant differences in the overall distribution of Sr-90 in the aquifer. This is apparent by comparing Figure J-8-19 to J-11-11 and noting that the decreased infiltration rate has reduced the spatial extent of Sr-90 in the 0.8 pC/L-8 pCi/L range north of the tank farm. As discussed in Appendix A, there is an apparent water divide near the tank farm in the 110 ft interbed. It slopes north nearer the Big Lost River, and slopes south near the tank farm. Reducing the overall infiltration in this case has prevented the higher Sr-90 concentrations from migrating to the north where they are driven downward by the high fluxes from the Big Lost River. Keeping the Sr-90 to the south where it moves slower allows it to decay more en route to the aquifer and has allowed the area above the MCL to be contained to a very small area just south of the tank farm in year 2095.

Peak aquifer concentrations for this simulation are shown in red and can be compared to the RI/BRA base case results shown in black on Figure J-11-12. The simulated Sr-90 concentrations were predicted to remain above the MCL from 1960 through year 2099. In the RI/BRA base case, the peaks in concentration that occur in the 2000-2005 time frame are a direct result of peak flows in the Big Lost River that drive Sr-90 from deep in the vadose zone. Those peaks are not present in this sensitivity case. However, in both cases, there is a noticeable step decrease in concentration that occurs following the removal of anthropogenic water at land surface in 2095. The predicted peak Sr-90 concentration in the year 2095 is 8.9 pCi/L, about twice as high as predicted for the RI/BRA base case (18.6 pCi/L).

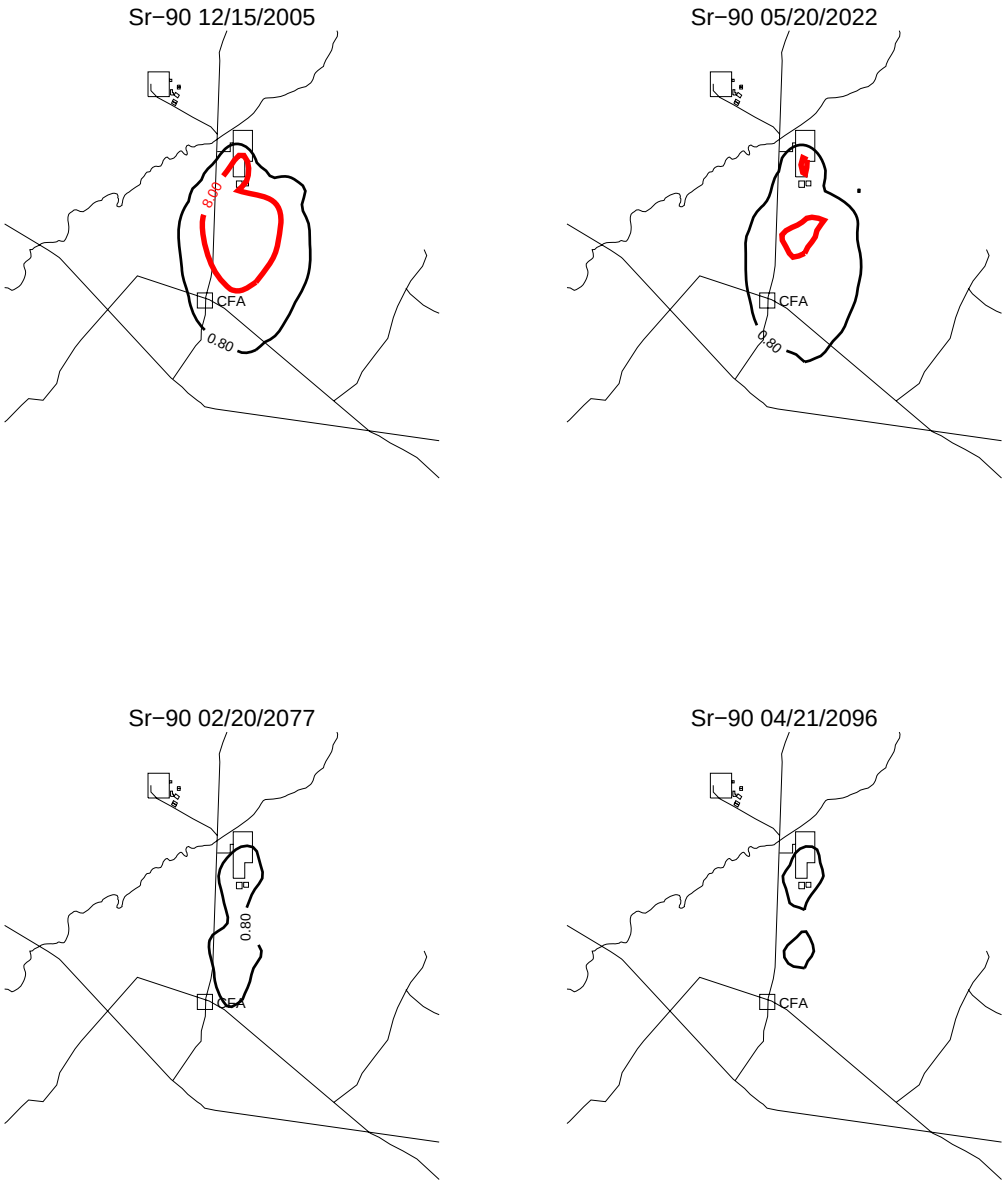

Figure J-11-10. Sr-90 aquifer concentration contours reducing infiltration in the tank farm to 3 cm/yr (pCi/L) (MCL = thick red line, 10*MCL = thin red line, MCL/10 = black line).

Figure J-11-11. Sr-90 aquifer concentration contours reducing infiltration in the tank farm to 3 cm/yr (pCi/L) (continued) (MCL = thick red line, 10*MCL = thin red line, MCL/10 = black line).

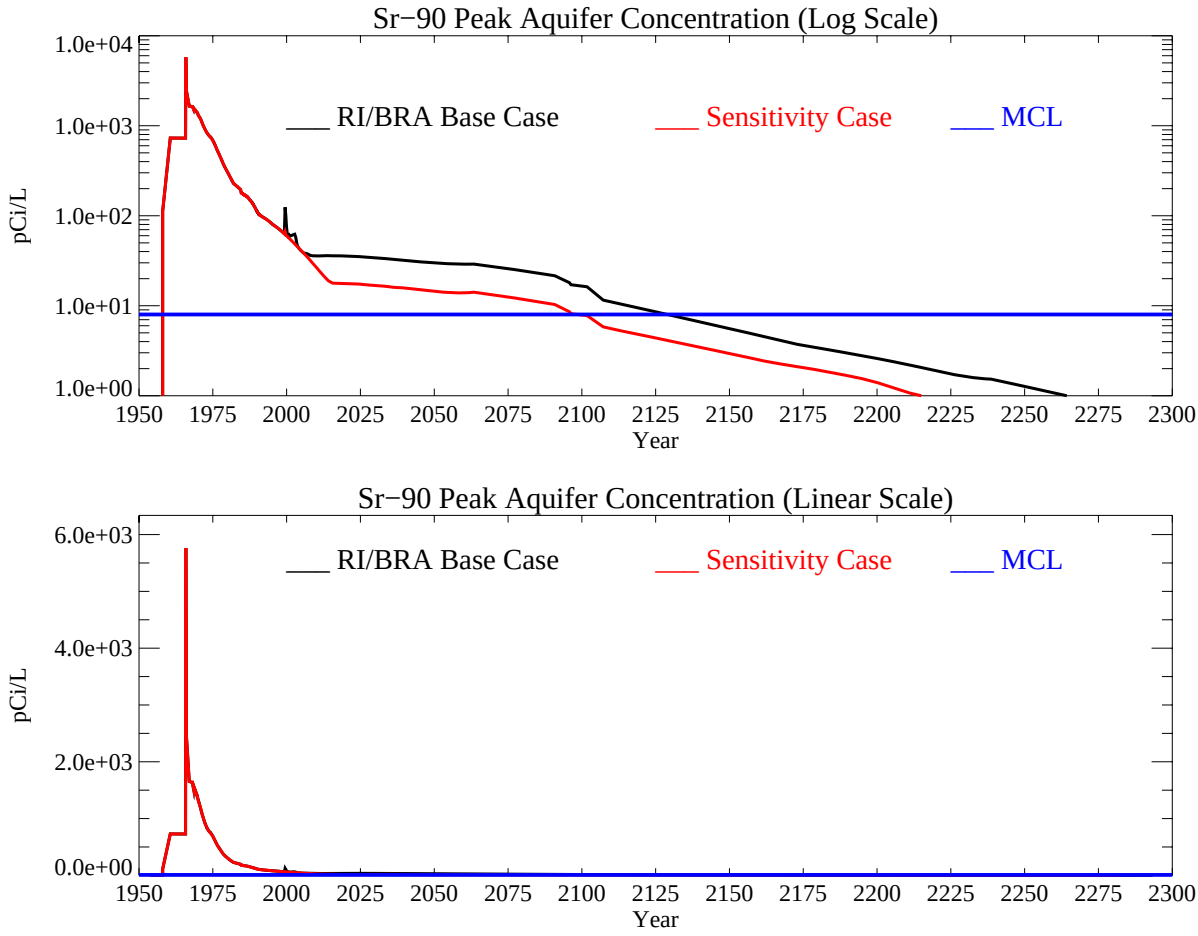

Figure J-11-12. Sr-90 peak aquifer concentrations reducing infiltration in the tank farm to 3 cm/yr (pCi/L) with the MCL in blue, RI/BRA model in black and this sensitivity run in red.

J-11.2 Higher 39 cm/yr Infiltration Through the Tank Farm Liner

It is not clear that the liner placed over the tank farm in 1977 is effective in reducing infiltration. As discussed in Appendix A, Section 3.3 and in Appendix B, some of the monitoring results suggest that it may be increasing local recharge in that area. This sensitivity simulation evaluates the transport assuming that 39 cm/yr infiltrates through the liner in the tank farm to account for that potential increase in infiltration rate. As with the first hydrologic sensitivity run, the rate was not changed until year 1977, and is representative of the total infiltration including that from anthropogenic losses and precipitation. The affected area corresponds to the 10 acres spanning the tank farm.

J-11.2.1 Geochemical Evolution in the Alluvium

An increase from 18 cm/yr to 39 cm/yr in infiltration rate after 1977 (5 years after the CPP-31 release) resulted in a rapid increase in SrCO3, and decrease in SrOH and Sr+ ion in the aqueous phase. The relative abundance of Sr+ ion is much larger than that of SrCO3 and SrOH, resulting in an overall decrease in aqueous phase Sr-90 concentrations with the increase in infiltration water. This is a result of increasing the incoming flux of Na, HCO3-, and Ca+2 ions that are contained in the infiltration water. Although, in the case of CPP-31, the competition effect for exchange sites resulted in more Sr-90 mobility, the influx of HCO3 results in increased buffer capacity. The pH of this resulting scenario is slightly higher than it was for the RI/BRA base case.

The amount of transported aqueous-phase Sr-90 (Figure J-11-13) is somewhat sensitive to this change in buffering capacity, and as a result, less Sr-90 leaves the alluvium in the first 20 years under this scenario than as predicted to occur in the absence of the slight increase in infiltration. After 5, 10, 15, and 20 years, the total Sr-90 that has entered the vadose zone under the alluvium is 1575, 5536, 5558, and 5580 Curies, respectively as shown in Figure J-11-13 (G). With this higher infiltration rate, a much larger fraction (10320 Ci vs. 3564 Ci) remains in the alluvium after 20 years as shown in the summary Figure J-11-13 (I).

The largest difference in the distribution of Sr-90, relative to the RI/BRA base case, occurs in the Sr-90 on the exchange sites and in the SrCO3 species. The change in Sr90 on exchange sites mirrors that in the SrCO3 species. Shortly after the increase in infiltration rate, there is a rapid increase in Sr-90 on the exchange sites. Because the majority of Sr-90 is in the adsorbed phase after the initial re-equilibration period, this increase is significant. The effective K_d is essentially the ratio of activity on the exchange sites to that in the aqueous phase. As the exchanged activity increases, and the aqueous phase Sr-90 concentrations decrease, the effective K_d increases. After 20 years, the effective K_d has approached an average value of 13 meq/L, which is much higher than that obtained in the RI/BRA base case.

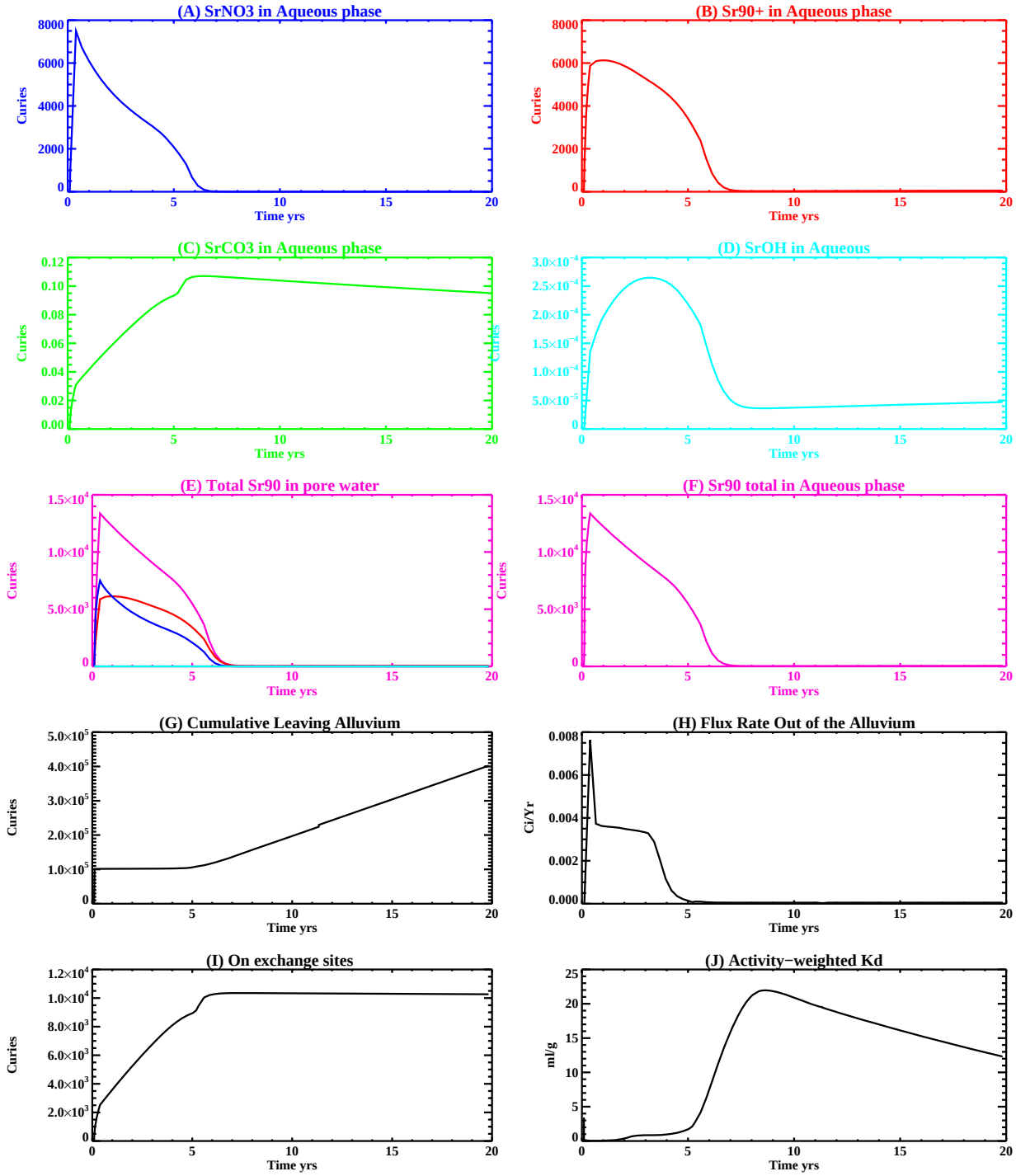

Figure J-11-13. Summary figure illustrating the speciation of Sr-90 in the aqueous phase (A-F), total Sr-90 in the pore-water of the alluvium (E), cumulative curies of Sr-90 having left the alluvium (G), flux rate leaving the alluvium (H), Sr-90 on the exchange sites (I), and effective partitioning coefficient (Kd) (J).